Static and dynamic properties of simulated liquid and amorphous GeO_2

2006 J. Phys.: Condens. Matter 18 777

(http://iopscience.iop.org/0953-8984/18/3/003)

INSTITUTE OF PHYSICS PUBLISHING JOURNAL OF PHYSICS: CONDENSED MATTER

J. Phys.: Condens. Matter **18** (2006) 777–786 doi:10.1088/0953-8984/18/3/003

Static and dynamic properties of simulated liquid and amorphous GeO_2

Vo Van Hoang

Department of Physics, College of Natural Sciences, HochiMinh City National University, 227 Nguyen Van Cu Street, Distr. 5, HochiMinh City, Vietnam

E-mail: vvhoang2002@yahoo.com

Received 13 September 2005, in final form 8 November 2005
Published 21 December 2005
Online at stacks.iop.org/JPhysCM/18/777

Abstract

Static and dynamic properties of liquid and amorphous GeO_2 have been simulated by a molecular dynamics method in a model containing 3000 particles under periodic boundary conditions. We have proposed for the first time new interatomic potentials for liquid and amorphous GeO_2 which have a Morse-type potential for short range interaction in the system. The structure of liquid and amorphous models is analysed through the partial radial distribution functions, coordination number distributions, interatomic distances and bond angle distributions. The calculated data for the structure and atomization energy of GeO_2 system agree well with the experimental ones. Further, for the first time, diffusion in liquid GeO_2 has been studied. We found that the temperature dependence of the diffusion constant D shows an Arrhenius law at temperatures above the melting point and it shows a power law, $D \propto (T - T_c)^\gamma$, at higher temperatures. The evolution of the structure upon cooling has been observed and presented.

1. Introduction

GeO_2 is a chemical and structural analogue of SiO_2; the two oxides have many similarities in structure and physical properties and they have considerable scientific interest and technological importance [1]. However, while liquid and amorphous SiO_2 have been under intensive investigation for the past few decades, there has been less attention paid to liquid and amorphous GeO_2. In recent years, great interest has focused on vitreous GeO_2, using a number of experimental methods such as the neutron diffraction [2, 3], high energy x-ray diffraction [4] and anomalous x-ray scattering at the germanium edge [5, 6] techniques, or using a combination of neutron diffraction, x-ray diffraction and anomalous x-ray scattering [7]. There is good agreement between experimental data for the structure of vitreous GeO_2. It was found that the mean interatomic distances were $r_{Ge-Ge} \approx 3.16$–3.18 Å, $r_{Ge-O} \approx 1.73$ Å and $r_{O-O} \approx 2.83$ Å (see [2–7]), while the mean bond angles $\theta_{O-Ge-O} = 109°$ and $\theta_{Ge-O-Ge} = 133°$

(see [8]) and the mean coordination number for the Ge–O and O–Ge pairs are equal to 4 and 2, respectively [2, 9]. This means that at ambient pressure, vitreous GeO_2 has a slightly distorted tetrahedral network structure like vitreous silica. However, more detailed information about the local structure of vitreous GeO_2 can be provided only by computer simulation. Due to lack of good interatomic potentials for liquid and amorphous GeO_2, we can find only a few simulation works on the structure of liquid and amorphous GeO_2. By using classical MD simulation, the structure of densified GeO_2 has been studied [10] in a model containing 768 particles with a Born–Huggins–Mayer-type potential which has been fitted to recover the crystalline phases of GeO_2 given by Oeffner and Elliot [11]. Calculations showed that the coordination number of Ge changes with increasing density and at ambient density, amorphous GeO_2 has a tetrahedral network structure like those observed in practice. A comparative numerical study of liquid GeO_2 and SiO_2 has been performed and it was found that the short range orders are identical in liquid and glass phases, made up of tetrahedral networks, while longer range order displays differences with temperature [12]. By using the same interatomic potentials, structural properties of liquid germania were investigated by Gutierrez and Rogan in a model containing 576 particles at 21 different densities [13]. Simulations showed that at ambient density there is short range order of a slightly distorted tetrahedral network like those obtained in the amorphous state. However, it seems that the simulation data in [10, 13] did not agree well with the experimental ones for the mean Ge–Ge interatomic distance; it was found that $r_{Ge-Ge} \approx 3.32$ Å in [10] and $r_{Ge-Ge} \approx 3.30$ Å in [13] versus the experimental value of around 3.16–3.18 Å. Moreover, the atomization energy of the model was not reported in these works.

Therefore, our aim here is to find new interatomic potentials which describe well both the structure and the atomization energy of liquid and amorphous GeO_2. We also study the evolution of the structure and diffusion in vitreous GeO_2 upon cooling in a large model containing 3000 particles.

2. Calculations

Simulations were performed at constant volume, corresponding to the real density of amorphous germania of 3.65 g cm^{-3}. We use the Verlet algorithm with the MD time step of 1.0 fs. Liquid and amorphous GeO_2 models were obtained by cooling from the melt. The initial model at the temperature of 5000 K was obtained by relaxing a random configuration of 3000 particles over 100 000 MD time steps. The temperature of the system decreases linearly over time as $T = T_0 - \gamma t$, where $T_0 = 5000$ K and the cooling rate $\gamma = 5 \times 10^{13}$ K s^{-1}. The so-obtained configurations at finite temperatures, by cooling from the melt, were subsequently relaxed for 25 ps before calculating static and dynamic properties. In order to calculate the coordination number distributions and bond angle distributions in liquid and amorphous GeO_2, we adopt the fixed values $R_{Ge-Ge} = 3.6$ Å, $R_{Ge-O} = 2.2$ Å and $R_{O-O} = 3.2$ Å. Here R is a cut-off radius which was chosen as a first minimum after a first peak in the partial radial distribution functions (PRDFs) of an amorphous model at the temperature of 300 K. We have proposed interatomic potentials for liquid and amorphous GeO_2, which have weak electrostatic interaction and Morse-type short range interaction as follows:

$$U_{ij}(r) = \frac{q_i q_j}{r} + D_0 \left\{ \exp\left[\gamma\left(1 - \frac{r}{R_0}\right)\right] - 2\exp\left[\frac{1}{2}\gamma\left(1 - \frac{r}{R_0}\right)\right]\right\} \qquad (1)$$

where q_i and q_j represent the charges of ions i and j, and after intensive testing we found the optimum value for charges of the ions in order to get good agreement with the experimental data for atomization energies of the system which are as follows: $q_{Ge} = +2.0e$ and $q_O = -1.0e$ (e is the elementary charge unit); these charges are close to those used in [11, 13] (i.e. equal

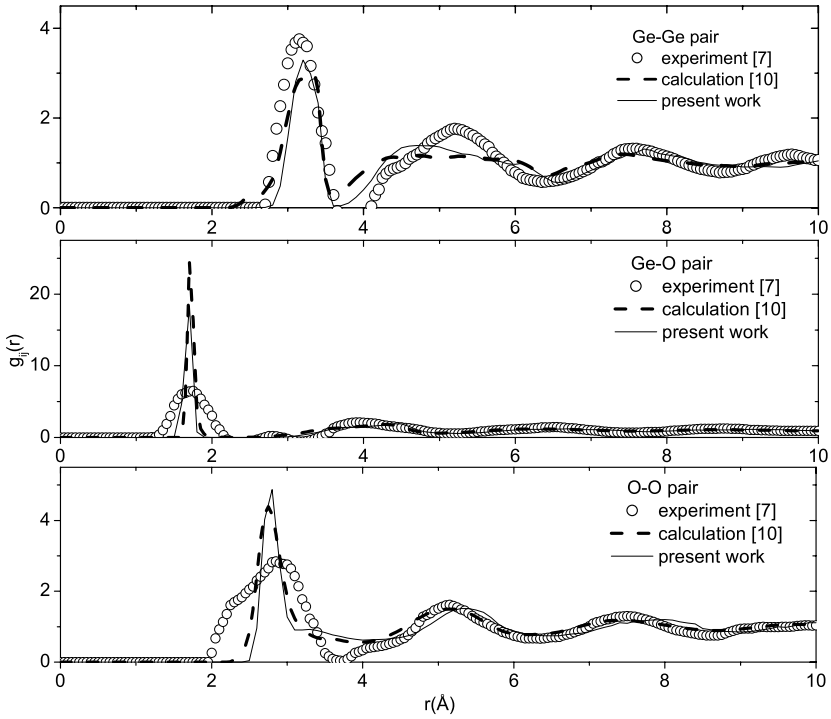

Figure 1. Partial radial distribution functions of an amorphous GeO_2 model at the temperature of 300 K.

to $+1.5e$ and $-0.75e$ for Ge and O, respectively); r denotes the interatomic distance between atoms i and j; the parameters of the Morse potentials are given below:

Interaction	D_0 (eV)	γ	R_0 (Å)
Ge–Ge	0.014	15.3700	3.600
Ge–O	3.700	8.6342	1.760
O–O	0.044	10.4112	4.400

Interatomic potentials of this type have been successfully used for simulating the structure and properties of vitreous silica [14, 15]. And due to the many similarities in structure and properties of vitreous GeO_2 and SiO_2, we have developed such potentials for our GeO_2 system by modifying the parameters of the potentials used in [14, 15] to get good agreement with the experimental data for the structure of liquid and amorphous GeO_2. The cut-off radius for the short range interaction is equal to half of the length of the main cube.

3. Results and discussion

3.1. Structural properties of liquid and amorphous GeO_2 (a-GeO_2)

The structural characteristics of the a-GeO_2 model obtained at the temperature of 300 K are in good accordance with the experimental data and with those calculated in [10] (see figure 1 and table 1). Moreover, our calculated mean interatomic distance r_{Ge-Ge} in a-GeO_2 is equal

Table 1. Structural characteristics of a-GeO_2. r_{ij}—positions of the first peaks in PRDFs; θ—the mean bond angle; Z_{ij}—the average coordination number (numbers 1 and 2 denote Ge and O, respectively).

	r_{ij} (Å)			Z_{ij}					
References	1–1	1–2	2–2	1–1	1–2	2–1	2–2	θ_{O-Ge-O}	$\theta_{Ge-O-Ge}$
Our cal. data for a-GeO_2 at 300 K	3.21	1.69	2.78	4.06	4.00	2.00	6.44	108°	133°
Cal. data for a-GeO_2 [10]	3.32	1.72	2.81		4.10				
Exp. data for a-GeO_2 [8]	3.16	1.73	2.83		4.00			109°	133°
Exp. data for a-GeO_2 [2, 9]	3.185	1.74	2.83		4.00	2.00			130°
Cal. data for a-SiO_2 [16]	3.16	1.60	2.59		4.00	2.00		108.3°	152°
Exp. data for a-SiO_2 [17]	3.12	1.62	2.65		4.00	2.00		109.5°	144°

to 3.21 Å and agrees well with the experimental one; the agreement is better than those obtained by simulation in [10, 13]. The calculated mean coordination numbers for Ge–O and O–Ge pairs are equal to 4 and 2, respectively, and these coincide with the experimental ones. Further, for an ideal tetrahedral network structure the O–Ge–O angle is 109.47°, O–O–O is 60° and Ge–O–O is equal to 35.26°. Our calculated O–Ge–O and Ge–O–Ge angles are equal to 108° and 133° and are in good accordance with the experiment. Combining such angles with the mean coordination numbers described above, we can conclude that a-GeO_2 has a slightly tetrahedral network structure and almost 99.9% of the Ge atoms are surrounded by four oxygen atoms, like in liquid and a-SiO_2. The same structure has been obtained for a liquid GeO_2 model at the temperature of 2000 K (not shown). More detailed information about local structure in the system can be found via the coordination number distributions and bond angle distributions. As shown in figure 2, the coordination number distributions in the amorphous state at the temperature of 300 K are similar to those of the liquid state presented in [13] with the exception of the O–O pair case, where the peak in our curve is located at the value of 6 versus 8 in [13]. The discrepancy might be related to the difference of the cut-off radii for the O–O pair used here and in [13]. There are no experimental data for Z_{O-O} in vitreous GeO_2. However, for a-SiO_2 the main peak in the coordination number distribution for the O–O pair is at 6 (see in [16]). And therefore, it seems that our data for the coordination number of the O–O pair are more reliable than those observed in [13]. Figure 3 shows that the main peaks of the Ge–Ge–Ge and O–O–O angle distributions are at 60° and 59°, respectively. Those for Ge–Ge–O and Ge–O–O angles are at 23° and 36°, slightly differ from those for the liquid state [13].

One more thing we would like to discuss here is the atomization energy of the system, which is often ignored in simulation work. The calculated total energy, with respect to free Ge^{2+} and O^{1-} ions at rest for our a-GeO_2 model at the temperature of 300 K, is $E_{ion} = -4307$ kJ mol^{-1}. We can recalculate the atomization energy using the equation $E_a = -E_{ion} - E_{trans} + E_{kin}$. Here E_{trans} is the energy spent in converting all free neutral atoms to free ions and E_{kin} is the kinetic energy of the particles. The energy of ionization of a neutral Ge atom to a Ge^{2+} ion is 23.8346 eV/atom; the electron affinity of the O atom is 6.76 eV/atom [18].

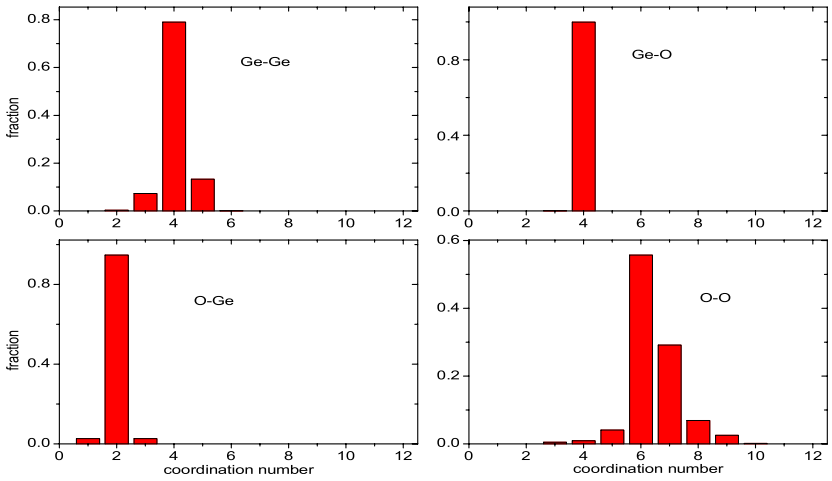

Figure 2. Coordination number distributions in the a-GeO_2 model obtained at the temperature of 300 K.

(This figure is in colour only in the electronic version)

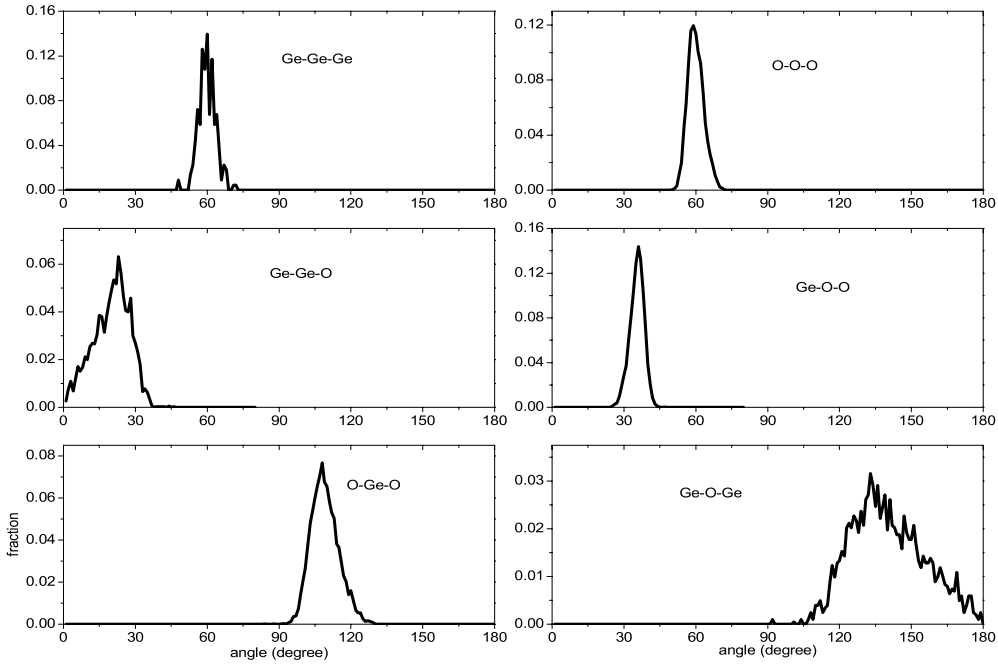

Figure 3. Bond angle distributions in the a-GeO_2 model obtained at the temperature of 300 K.

Therefore, the atomization energy is $E_a \approx 1355$ kJ mol^{-1} (per mole of GeO_2 molecules), while the experimental value for crystalline GeO_2 is equal to 1455 kJ mol^{-1} [18]. This means that the calculated atomization energy of a-GeO_2 is close to the experimental one for the crystalline phase. The calculated atomization energy of a-GeO_2 is less than that of the crystalline phase at 100 kJ mol^{-1}, which can be considered a heat of crystallization of a-GeO_2. There are no

Table 2. Temperature dependence of the coordination number distribution Z_{Ge-O} for the Ge–O pair in GeO_2 models.

Z_{Ge-O}	1	2	3	4	5
Number of Ge^{2+} ions ($T = 5000$ K)	0	1	138	857	4
Number of Ge^{2+} ions ($T = 4500$ K)	0	1	96	902	1
Number of Ge^{2+} ions ($T = 4250$ K)	0	1	57	939	3
Number of Ge^{2+} ions ($T = 4000$ K)	0	0	57	943	0
Number of Ge^{2+} ions ($T = 3750$ K)	0	0	43	956	1
Number of Ge^{2+} ions ($T = 3500$ K)	0	0	35	965	0
Number of Ge^{2+} ions ($T = 3000$ K)	0	0	26	974	0
Number of Ge^{2+} ions ($T = 2500$ K)	0	0	4	996	0
Number of Ge^{2+} ions ($T = 2000$ K)	0	0	9	991	0
Number of Ge^{2+} ions ($T = 300$ K)	0	0	1	999	0

experimental data for the heat of crystallization of a-GeO_2; however, for amorphous oxides it is often equal to a few hundreds of kJ mol^{-1} [19]. It is interesting to compare the structures of a-SiO_2 and a-GeO_2. Calculations show that the structures of these oxides are very similar; however, one can see that the mean Si–O–Si bond angle is much larger than the Ge–O–Ge one, implying that a-SiO_2 is looser than a-GeO_2. One can check the topological looseness of a system directly via the parameter ρ_1 which is defined as the mean height of the first peaks in PRDFs [19]:

$$\rho_1 = \frac{\sum X_i X_j r_{ij}}{d_0}. \tag{2}$$

Here X_i and X_j are the atomic parts of the components in the system and r_{ij} is the position of the first peak in the PRDFs; the summation is over all pairs of particles and $d_0 = (V/N)^{1/3}$, where N is the number of particles in volume V. Topologically dense systems have $\rho_1 = 1.08 \pm 0.02$ and loose systems have $\rho_1 < 1.05$. From the calculated data shown in table 1, for a-GeO_2 the parameter ρ_1 is equal to 0.78. This means that a-GeO_2 is a loose system.

3.2. Evolution of structure upon cooling

According to the diffraction and to the calculated data presented above, liquid and a-GeO_2 have a slightly distorted tetrahedral network structure with the main structural unit GeO_4 and the mean coordination numbers $Z_{Ge-O} = 4$ and $Z_{O-Ge} = 2$. This means that the serious defects in the model can be considered as the Ge atoms with $Z_{Ge-O} = 3$ or O atoms with $Z_{O-Ge} = 1$ or 3. Therefore, it is interesting to study the evolution of coordination number distributions for the Ge–O and O–Ge pairs upon cooling from the melt in order to detect the temperature dependence of the structural defects. As shown in table 2, the number of defects with $Z_{Ge-O} = 3$ decreases upon cooling. The number of defects with $Z_{O-Ge} = 1$ decreases upon cooling down to $T = 2500$ K and then it slightly increases; meanwhile the number of defects with $Z_{O-Ge} = 3$ decreases upon cooling down to $T = 3750$ K and then it also slightly increases (not shown).

Calculations showed that the probability for the occurrence of structural defects in vitreous SiO_2 is described well by an Arrhenius law [20]:

$$P_{ij} = A_{ij} \exp(-E_{ij}/T). \tag{3}$$

Here P_{ij} denotes the probability that an ion of type i has exactly Z nearest neighbours of type j. Figure 4 shows that the probability for defects with $Z_{Ge-O} = 3$ and $Z_{O-Ge} = 1$ also

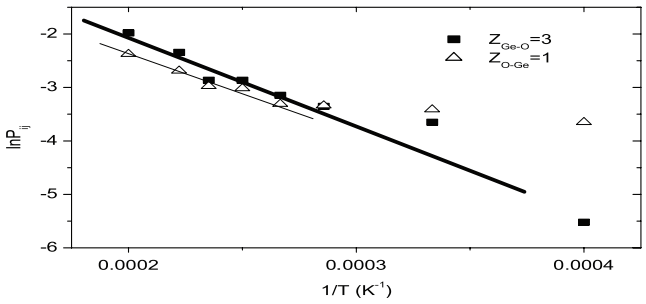

Figure 4. Temperature dependence of the probability for the occurrence of defects, P_{ij}, with the coordination numbers $Z_{Ge-O} = 3$ and $Z_{O-Ge} = 1$ (due to the small number of points for $Z_{O-Ge} = 3$, it has not been presented in the figure).

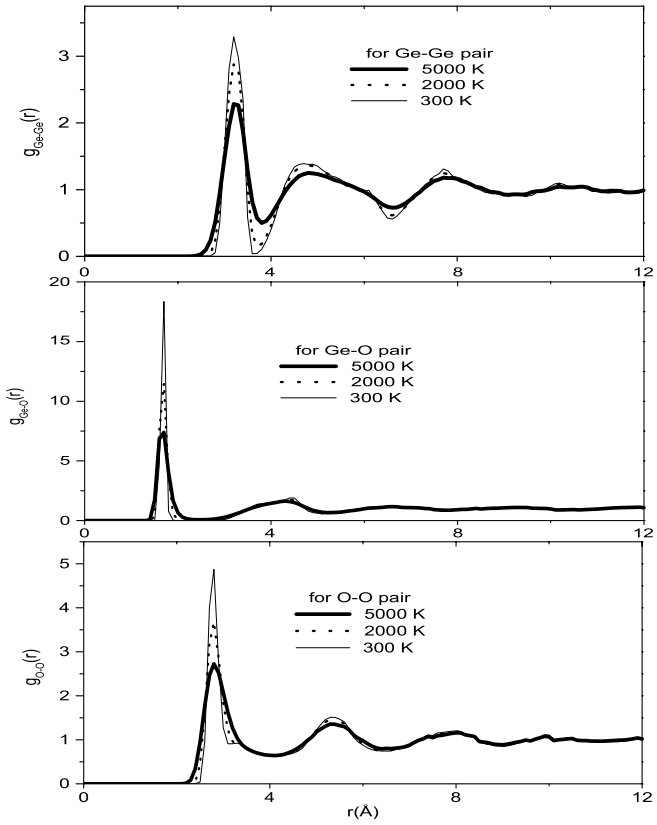

Figure 5. Radial distribution functions of the GeO_2 system upon cooling.

shows an Arrhenius law at temperatures above 3500 K. Prefactors A_{ij} and activation energies E_{ij} were found: $A_{Ge-O} = 3.139$ and $E_{Ge-O} = 16\,038$ K for $Z_{Ge-O} = 3$; $A_{O-Ge} = 0.988$ and $E_{O-Ge} = 11\,632$ K for $Z_{O-Ge} = 1$. These values differ from those observed for silica melt [20].

In order to observe the evolution of the structure upon cooling, we also display PRDFs, $g_{ij}(r)$, for Ge–Ge, Ge–O and O–O pairs in relaxed models at the three different temperatures of 5000, 2000 and 300 K (figure 5). We can see that PRDFs strongly depend on the temperature

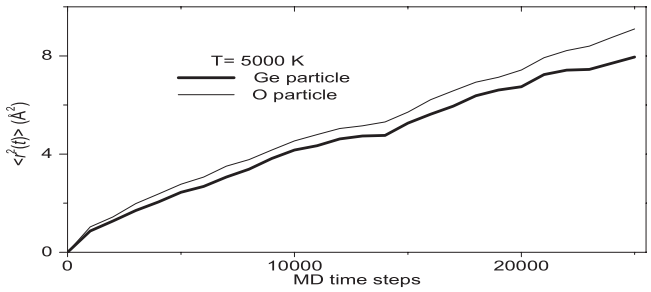

Figure 6. Time dependence of the mean square atomic displacement $\langle r^2(t)\rangle$ in the GeO_2 model obtained at the temperature of 5000 K.

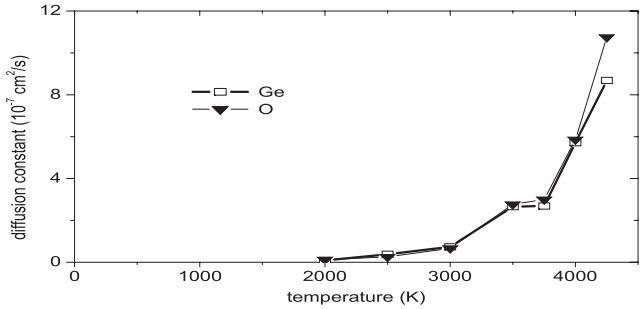

Figure 7. Temperature dependence of the diffusion constant D.

that the height of the individual peaks and minima become more pronounced upon cooling. And the most prominent changes have been observed for the first peak in $g_{ij}(r)$. The same phenomenon has been observed in vitreous silica [16].

3.3. Diffusion

By using the Einstein relation, $\lim_{t\to\infty} \frac{\langle r^2(t)\rangle}{6t} = D$, one can calculate the diffusion constant D via the mean square atomic displacement $\langle r^2(t)\rangle$ (see figure 6). And from the temperature dependence of the diffusion constant presented in figure 7, we can determine approximately the glass transition temperature T_g by extrapolation to $D = 0$, which is at around 1000 K. This value is close to the value of 1010 K reported in [10]; however, this is larger than those observed in practice, $T_g \approx 800$ K [21]. And according to our calculations, the diffusion constants for Ge and O particles in liquid GeO_2 are smaller than those of Si and O particles in silica melt at the same temperatures [20]. It is essential to note that the melting temperature of GeO_2 is equal to $T_m = 1378$ K and for silica the values are $T_g \approx 1500$ K and $T_m = 1995$ K (see in [13]). The temperature dependence of the diffusion constant for particles in the germania melt show an Arrhenius law at temperatures above the melting point with activation energies 1.12 and 0.83 eV for Ge and O, respectively. These values are smaller than those for silica (i.e. 4.66 and 5.18 eV for Si and O, respectively [20]). At higher temperatures, the curves deviate from an Arrhenius law (see figure 8) like those observed for silica melt [20]. And after intensive testing, we found that at high temperatures a power law like that given below is shown [20]:

$$D \propto (T - T_c)^{\gamma}. \tag{4}$$

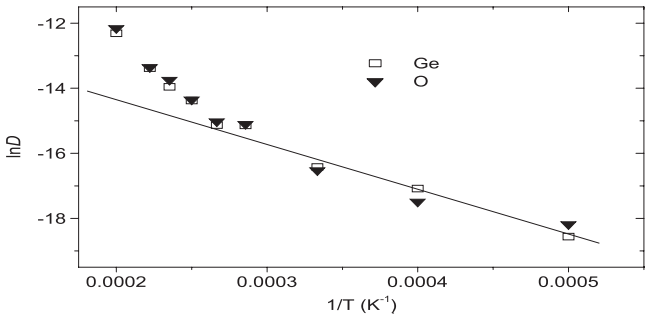

Figure 8. The $1/T$ dependence of ln D.

Here T_c is the critical mode-coupling theory temperature for germania which is estimated at about 3500 K and the exponent $\gamma = 1.506$ and 1.525 for Ge and O, respectively. For silica melt, $T_c = 3330$ K and $\gamma = 2.15$ and 2.05 for Si and O, respectively [20].

4. Conclusions

We draw the following conclusions:

(i) For the first time, we have proposed new interatomic potentials for liquid and amorphous GeO_2 which have weak electrostatic interaction and Morse-type short range interaction. These potentials describe well both the structure and atomization energy of the system.
(ii) Calculations show that liquid and a-GeO_2 have a slightly distorted tetrahedral network structure, like silica.
(iii) For the first time, the diffusion in liquid germania has been calculated and the temperature dependence of the diffusion constant shows an Arrhenius law at temperatures above the melting point and shows a power law, $D \propto (T - T_c)^{\gamma}$, at higher temperatures, like silica melt. The critical mode-coupling theory temperature T_c for germania was determined as about 3500 K, and the exponent γ is equal to 1.50 for both Ge and O. The glass transition temperature T_g for the GeO_2 system is around 1000 K.

Acknowledgment

The author thanks Dr M Micoulaut for providing his own calculation data for PRDFs in order to compare with the ones of the present work.

References

[1] Vogel W 1994 *Glass Chemistry* (Berlin: Springer)
[2] Desa J A E, Wright A C and Sinclair R N 1988 *J. Non-Cryst. Solids* **99** 276
[3] Waseda Y, Sugiyama K, Matsubara E and Harada K 1990 *Mater. Trans. JIM* **31** 421
[4] Neuefeind J and Liss K D 1996 *Ber. Bunsenges Phys. Chem. Chem. Phys.* **100** 1341
[5] Bondot P 1974 *Phys. Status Solidi* a **22** 511
[6] Price D L, Ellison A J G, Saboungi M L, Hu R Z, Egami T and Howells W S 1997 *Phys. Rev.* B **55** 11249
[7] Price D L, Saboungi M L and Barnes A C 1998 *Phys. Rev. Lett.* **81** 3207
[8] Tsiok O B, Brazhkin V V, Lyapin A G and Khvostantsev L G 1998 *Phys. Rev. Lett.* **80** 999
[9] Hussin R, Dupree R and Holland D 1999 *J. Non-Cryst. Solids* **246** 159

[10] Micoulaut M 2004 *J. Phys.: Condens. Matter* **16** L131
[11] Oeffner R D and Elliott S R 1998 *Phys. Rev.* B **58** 14791
[12] Micoulaut M 2004 *Chem. Geol.* **213** 197
[13] Gutierrez G and Rogan J 2004 *Phys. Rev.* E **69** 031201
[14] Huff N T, Demiralp E, Cagin T and Goddard W A III 1999 *J. Non-Cryst. Solids* **253** 133
[15] Takada A, Richet P, Catlow C R A and Price G D 2004 *J. Non-Cryst. Solids* **345/346** 224
[16] Vollmayr K, Kob W and Binder K 1996 *Phys. Rev.* B **54** 15808
[17] Mozzi R L and Warren B E 1969 *Acta Crystallogr.* **2** 164
[18] Lide D R (ed) 1996 *CRC Handbook of Chemistry and Physics* (New York: CRC Press)
[19] Belashchenko D K 1997 *Russ. Chem. Rev.* **66** 733
[20] Horbach J and Kob W 1999 *Phys. Rev.* B **60** 3169
[21] Meyer A, Schober H and Neuhaus J 2001 *Phys. Rev.* B **63** 212202